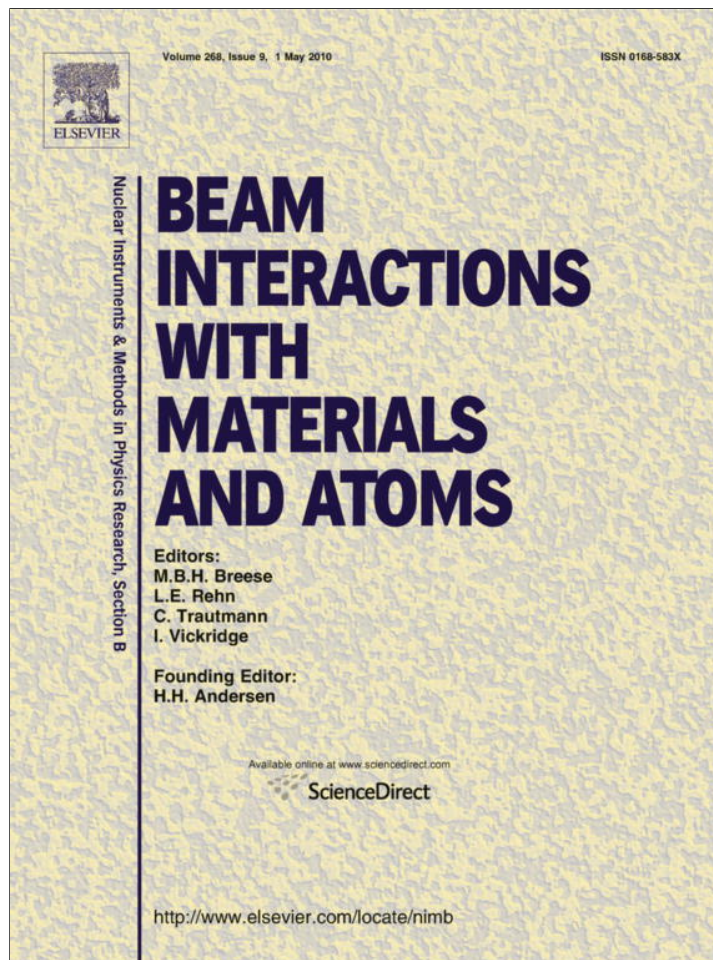


Provided for non-commercial research and education use.  
Not for reproduction, distribution or commercial use.



This article appeared in a journal published by Elsevier. The attached copy is furnished to the author for internal non-commercial research and education use, including for instruction at the authors institution and sharing with colleagues.

Other uses, including reproduction and distribution, or selling or licensing copies, or posting to personal, institutional or third party websites are prohibited.

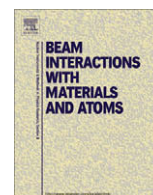
In most cases authors are permitted to post their version of the article (e.g. in Word or Tex form) to their personal website or institutional repository. Authors requiring further information regarding Elsevier's archiving and manuscript policies are encouraged to visit:

<http://www.elsevier.com/copyright>



Contents lists available at ScienceDirect

## Nuclear Instruments and Methods in Physics Research B

journal homepage: [www.elsevier.com/locate/nimb](http://www.elsevier.com/locate/nimb)

# Micromachining of amplitude and phase modulated reflective computer generated hologram patterns in silicon

Y.S. Ow<sup>a,\*</sup>, M.B.H. Breese<sup>a</sup>, Y.R. Leng<sup>a</sup>, S. Azimi<sup>a</sup>, E.J. Teo<sup>a</sup>, X.W. Sun<sup>b</sup>

<sup>a</sup>Physics Department, National University of Singapore, Lower Kent Ridge Road, Singapore 119260, Singapore

<sup>b</sup>School of Electrical and Electronic Engineering, Nanyang Technological University, Nanyang Avenue, Singapore 639798, Singapore

## ARTICLE INFO

### Article history:

Received 6 January 2010

Available online 20 January 2010

### Keywords:

Silicon  
Micromachining  
Computer generated holograms  
Holography  
Ion beam irradiation

## ABSTRACT

Silicon has been machined on lateral resolutions of micrometers and on depth resolutions of nanometers using a recently-developed process based on ion irradiation and electrochemical anodisation. Here we investigate its use as a recording medium for computer generated hologram patterns. We describe the fabrication of both amplitude and phase binary modulated reflective computer generated hologram patterns on a silicon surface with pixel sizes of 5  $\mu\text{m}$ . We further discuss the use of micromachined silicon to variably modulate both amplitude and phase in a continuous, rather than a binary fashion.

© 2010 Elsevier B.V. All rights reserved.

## 1. Introduction

### 1.1. Computer generated holography (CGH)

CGH hologram differs from conventional holography in that they are described mathematically by computing the phase and amplitude information of the wave propagation produced by an object, rather than physically recording it. There are many applications which use CGH, such as diffractive-optical elements for storage of digital data and images [1], precise interferometric measurements [2], pattern recognition [3], data encryption [4] and three-dimensional displays [5]. One advantage over conventional holograms produced by optical means is that the object used for recording CGH holograms does not need to exist as it may be described mathematically. Methods of calculating CGH patterns include Ray Tracing [6,7] and the Fourier Transform [8,9] method, which is used for the work described here.

### 1.2. Amplitude and phase modulation for image reconstruction

After a CGH hologram is computed, it has to be recorded onto a medium that is able to modulate the interference pattern from a coherent light source to produce a reconstructed image. Many different materials have been used to record CGHs, such as photorefractive materials like BaTiO<sub>3</sub> [10] and Fe-doped LiNbO<sub>3</sub> [11], photopolymers [12] and thermo-plastics [13].

\* Corresponding author. Tel.: + 65 65164135.

E-mail address: [g0601170@nus.edu.sg](mailto:g0601170@nus.edu.sg) (Y.S. Ow).

Generally, these materials have physical properties which enable them to modulate either the phase or the amplitude of the incoming light, but not both. Phase modulation is usually done by changing the optical thickness through which light has to travel, while amplitude modulation is carried by varying intensities of light passing through for transmission CGH, or reflected for reflective CGH. CGH devices based on liquid crystal spatial light modulators have also been reported [14]. To date, they are the only devices which are able to modulate both phase and amplitude [15], but their pixel resolution is usually in the range of tens of microns. A switchable phase modulated CGH using polymer-dispersed liquid crystals and a cell with patterned electrodes was reported with 50  $\mu\text{m}$  pixel sizes [16]. We recently demonstrated that CGH patterns with pixel sizes of about 5  $\mu\text{m}$  could be fabricated in thick poly (methyl methacrylate) (PMMA) layers using direct proton beam writing [17]. When filled with liquid crystals these thick patterns could be used for electrically switchable CGH patterns with 5  $\mu\text{m}$  pixel sizes [18].

### 1.3. Silicon micromachining using ion irradiation and electrochemical anodisation

Porous silicon is commonly used as a sacrificial material for micromachining silicon [19,20]. More recently, a new method of Si micromachining has been developed, based on irradiation with energetic ions, typically protons and helium ions, focused by a quadrupole lens system [21]. Such direct proton beam writing (PBW) produces point defects along the ion trajectories which locally increase the resistivity of p-type Si [22]. The irradiated wafer

is then electrochemically anodized in a hydrofluoride (HF) electrolyte. On applying a bias, an electrical current of holes travels to the wafer surface and porous silicon (PSi) starts to form at a rate proportional to the hole current density [23]. The hole current density flowing through the irradiated regions is reduced because the resistivity is increased, so anodisation occurs at a reduced rate. The PSi is easily removed with potassium hydroxide (KOH), revealing the irradiated Si surface relief structures. Various structures have been micromachined using this method, including tunable Distributed Bragg Reflectors [24], silicon waveguides [25], micro-turbines [26], variable wavelength and intensity of photoluminescence [27,28] and it has also been shown that gallium arsenide wafers behave in a similar manner [29,30].

More recently, a process which uses ion irradiation to micromachine Si on a micrometer lateral scale over wafer areas of several square centimeters was demonstrated [31], and this facility is used in the present work. A quadrupole lens system is used to project a uniform distribution of MeV ions over several square centimeters on wafer surface which is coated with a patterned photoresist which shields selective areas from ion irradiation. Together with electrochemical anodisation, this technique enables the rapid production of high-density arrays of a variety of optical and photonic components in Si.

#### 1.4. Silicon as a recording medium

It is difficult to record CGH patterns with variable pixel modulation to amplitude and phase, so existing recording techniques, using photolithography for example, usually modulate in an on/off binary manner. While it is possible to make CGH patterns with electron beam lithography at very high spatial resolutions of 10 nm, this is

also limited to a binary fashion rather than differing degrees of response of individual pixels. Moreover, most existing CGH recording media are usually only able to modulate either the phase or the amplitude but not both. In this work, we demonstrate the ability to modulate both the amplitude and phase using micromachined Si surfaces. In addition, we demonstrate the possibility of this approach for variable phase and amplitude modulation.

## 2. Experimental details

Moderately doped, 0.02  $\Omega$  cm p-type Si wafers are used here as we have previously shown that their rate of anodisation can

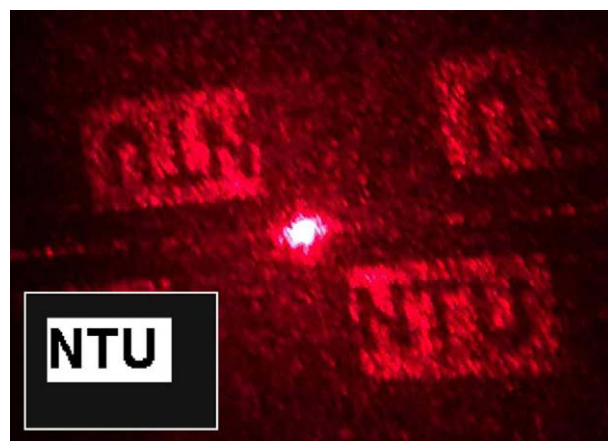


Fig. 2. Reconstructed image from the binary phase CGH in Fig. 1. The inset shows the encoded image of the letters "NTU".

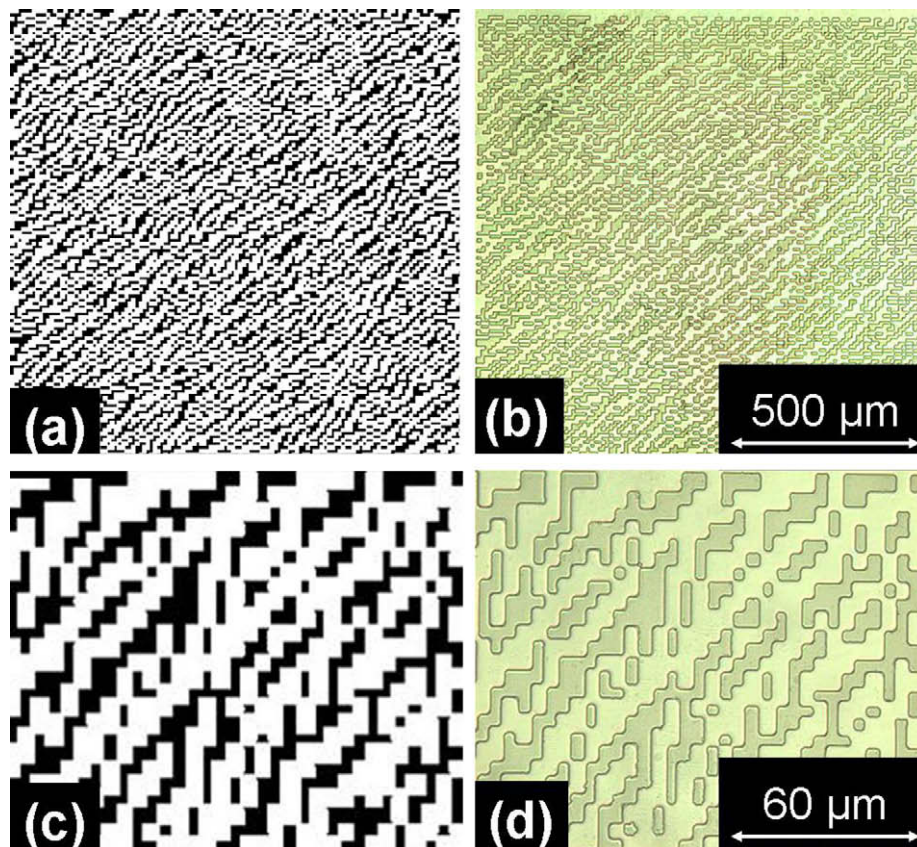


Fig. 1. (a) Binary phase CGH pattern consisting of  $1024 \times 1024$  pixels. (b) Optical image of the silicon surface relief pattern. The total area of the CGH on the Si is  $1 \times 1$  mm while the smallest features are about  $4 \times 4$   $\mu$ m. Panels (c) and (d) are enlarged images of the CGH pattern of the corresponding optical image on silicon.

be controlled over a wider range by varying the irradiation fluence [24]. Wafers were coated with hexamethyldisilazane (HMDS) by vapor priming to create adhesion between the sample and photoresist. A  $7\ \mu\text{m}$  thick photoresist, AZ p4620, was spin-coated onto the wafer and then pre-baked to  $95\ ^\circ\text{C}$  for 4 min. A chrome mask containing the computed CGH patterns was fabricated by laser lithography and transferred to the photoresist by standard UV photolithography resulting in two-step (resist and silicon step) binary CGH pattern on the photoresist. The sample was then exposed to a 600 keV helium ion beam which was uniformly distributed over an area of  $1.5 \times 1.5\ \text{cm}$ . Helium ions were used owing to their greater defect generation rate compared with protons, hence shorter irradiation time. Helium ions (600 keV) have a range of 4.0 and  $2.3\ \mu\text{m}$  in photoresist and silicon respectively, so the photoresist is thick enough to prevent irradiation induced-damage to the underlying silicon. The fluence was  $5 \times 10^{14}$  ions/cm<sup>2</sup>, high enough to greatly reduce the subsequent rate of PSi formation in silicon. In this way, no defects are introduced to the un-exposed/un-irradiated areas and during the subsequent anodisation step the PSi formation rate is not reduced in these areas compared to the irradiated regions. For a typical beam current of 100 nA the irradiation time for each sample was about 30 min. After irradiation, the photoresist layer was removed using nanostripper and the wafer anodized at a current density of  $70\ \text{mA}/\text{cm}^2$ . Finally, the wafer was immersed in KOH solution to remove the PSi layer, leaving behind a micromachined two-step silicon binary surface relief CGH pattern. Image reconstruction was carried out by reflecting a 5 mW red (650 nm) laser off the CGH patterns onto a viewing screen.

### 3. Binary phase and amplitude CGH patterns in silicon

Fig. 1(a) shows a binary phase CGH pattern of the letters NTU comprising  $1024 \times 1024$  black and white pixels. Fig. 1(b) shows an optical image of the binary phase CGH pattern in Fig. 1(a) transferred onto Si as described above. Binary phase modulation is achieved by the two micromachined step heights; the higher steps are the irradiated regions while the lower steps are the unirradiated regions where the anodisation rate is higher. These irradiated and unirradiated regions correspond to the black and white pixels in Fig. 1(a) respectively. From atomic force microscope (AFM) measurements, the difference in step height is approximately 700 nm. This causes incoming light to travel through different optical path lengths, hence modulating the phase. Fig. 1(c) and (d) are enlarged images of the generated CGH and the optical image of the CGH pattern on silicon respectively. The smallest feature size on the sample is  $4 \times 4\ \mu\text{m}$ . Good pattern transfer is achieved, demonstrating the precision and accuracy that may be achieved, resulting in a good reconstructed binary image in Fig. 2.

Fig. 3(a) shows a binary amplitude CGH made up of  $300 \times 300$  black and white pixels. The CGH pattern was transferred into silicon over an area of  $1.5 \times 1.5\ \text{mm}$ , with a pixel size of  $5 \times 5\ \mu\text{m}$ . There are two distinct intensities of reflected light which differ by 30% as measured from a line profile using a microscope, resulting in modulation of the amplitude of incoming light. The irradiated regions (black pixels) are less reflective while the unirradiated regions (white pixels) are more reflective owing to a variety of factors discussed below. Good pattern transfer is again observed, resulting in a good reconstructed image in Fig. 3(d).

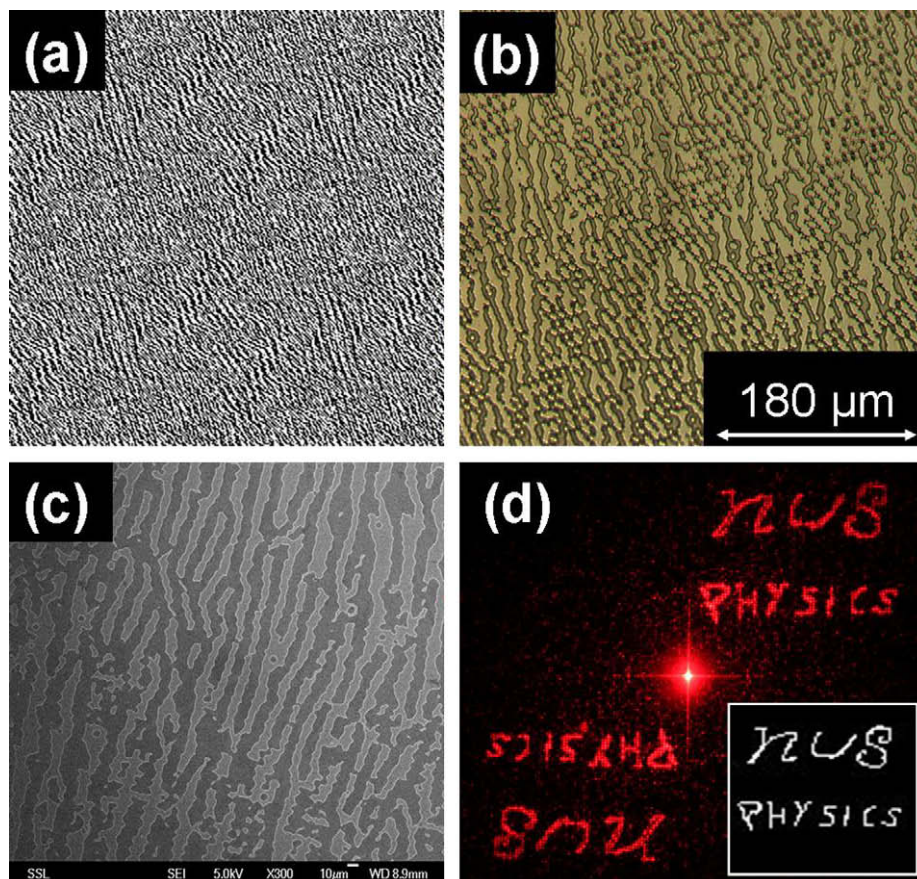


Fig. 3. (a) Binary amplitude CGH pattern consisting of  $300 \times 300$  pixels. Panels (b) and (c) respectively show an optical and SEM image of part of the transferred CGH pattern in silicon. (d) Reconstructed image of a phase CGH. Inset shows the original encoded image.

Fig. 3 demonstrates that silicon may be used for binary type amplitude CGH to produce binary type reconstructed images. We have also fabricated binary amplitude reflective CGH patterns capable of producing grayscale reconstructed images. Fig. 4(a) inset shows the encoded image in which each letter in the words “gray scale” has differing intensity. The reconstructed image in Fig. 4(a) exhibits the differing intensities reasonably well, as do the other reconstructed grayscale images in Fig. 4.

#### 4. Silicon as a material for producing continuously variable amplitude and phase CGH

We have demonstrated that silicon can be machined to give sufficient differences in reflective intensity and phase to produce binary reconstructed CGH images. Here we show that silicon can be continuously machined in both pixel height and reflectivity, allowing the generation of better quality reconstructed holograms [32] in conjunction with suitable CGH patterns.

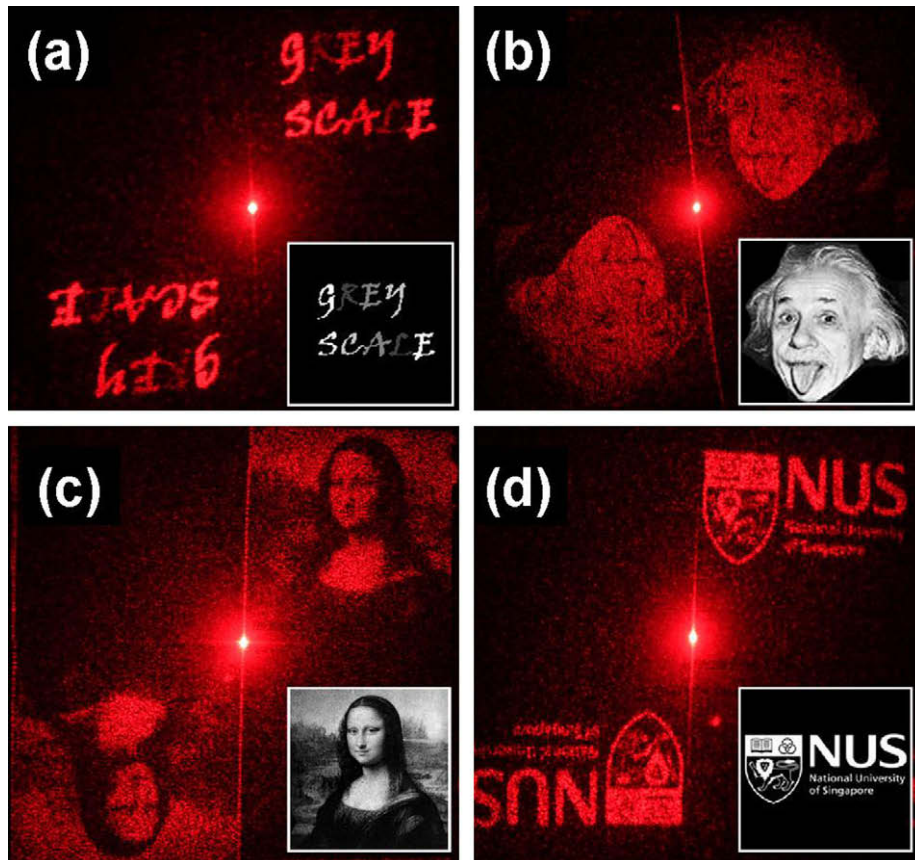


Fig. 4. Grayscale reconstructed images from binary amplitude CGH patterns on Si, with the original encoded images shown in the insets. (a) The letters “gray” has the letters “g”, “r”, “e” and “y” in 100%, 25%, 50% and 75% intensity respectively. (b)–(d) Grayscale reconstructed images of Albert Einstein, the Mona Lisa and logo of the National University of Singapore.

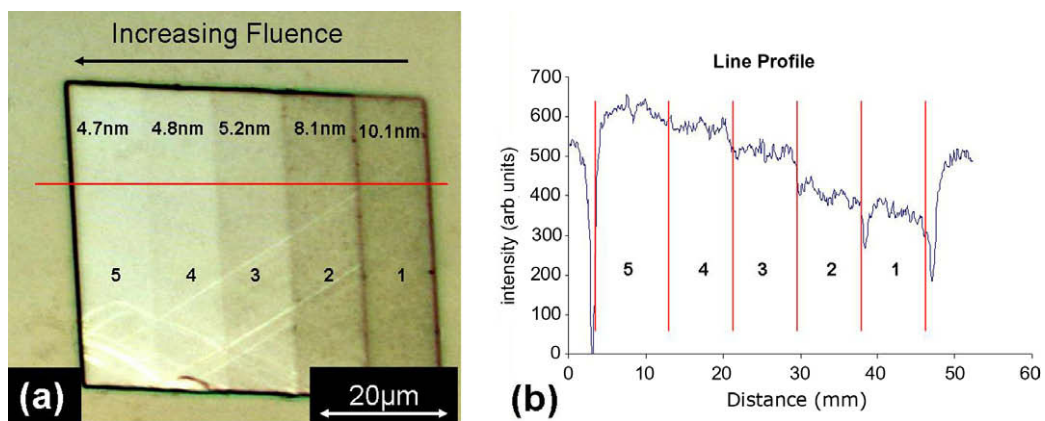
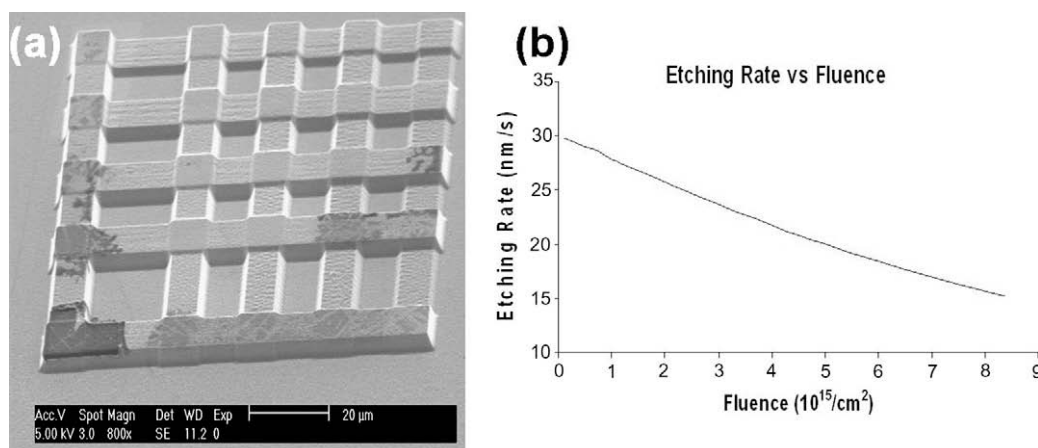


Fig. 5. (a) Optical image of surface relief Si with five lines 10 μm in width irradiated with increasing fluence from 1 to  $5 \times 10^{15}/\text{cm}^2$ , in increments of  $1 \times 10^{15}/\text{cm}^2$  AFM measurements of the roughness of each line is indicated. (b) Horizontal line profile across the irradiated lines at the location indicated in by the red line in (a) showing large variations in reflected intensity from white light. (For interpretation of the references to colour in this figure legend, the reader is referred to the web version of this article.)



**Fig. 6.** (a) SEM image of the surface relief of a silicon wafer which was irradiated in a cross hatched manner, producing steps of many different heights. (b) Plot of the relationship between the anodisation rate and fluence.

Five 10 μm wide lines were irradiated with 2 MeV proton fluences from 1 to 5 × 10<sup>15</sup>/cm<sup>2</sup>, in increments of 1 × 10<sup>15</sup>/cm<sup>2</sup> from right to left. The wafer was then anodized to a depth of 700 nm and the PSi removed. Fig. 5(a) shows variation in the reflectivity of the remaining silicon surface, with reflectivity clearly increasing with fluence. A line profile across the five lines is shown in Fig. 5(b) and shows distinct levels of reflectivity for each fluence, with the reflected intensity varying up to 50%. AFM measurements for the roughness of each line demonstrate that it decreases with fluence. However, the roughness variation would only result a change in reflectivity of 1–2%. Irradiated areas result in less current flowing through them during anodisation, consequently the porosity of the PSi at these regions is lower. Hence, we attribute the large observed variation in reflectivity to greater difficulty in removing the PSi of lower porosity from the irradiated surfaces and preferential ambient oxidation of the rougher surfaces, hence a lower reflectivity. This demonstrates that our silicon micromachining process is not limited to modulating the amplitude of light in a binary fashion, but is able to variably modulate the amplitude of incoming light over a wide range.

We have also irradiated five vertical bars using PBW using 2 MeV protons. Each bar was 10 × 100 μm, with fluences increasing from 2, 4, 6, 8, and 10 × 10<sup>15</sup> protons/cm<sup>2</sup>. The area was overlapped with similarly irradiated horizontal bars, resulting in a checker board image. The sample was then etched at 12 mA/cm<sup>2</sup> for 4 min and the PSi removed. The anodisation rate reduces with fluence, as shown in Fig. 6(b), producing increasing step height of the surface relief pattern. Incoming light is reflected through different optical path lengths due to the differing heights, hence variably modulating the phase rather than just in a binary fashion.

## 5. Conclusions

We have demonstrated the ability to fabricate binary phase and amplitude CGH patterns on silicon which gives rise to good reconstructed images. In addition, we also showed that these binary CGH are able to produce good grayscale reconstructed images. Together with an appropriate CGH generating software, this work shows that it is possible to use silicon as a recording medium to variably modulate amplitude and phase by having varying reflectivity and step heights respectively.

## Acknowledgement

Funding support by the Singapore Ministry of Education Academic Research Fund Tier 2 under Grant No. T207B1110 is acknowledged.

## References

- [1] W.L. Wilson, K. Curtis, M. Tackitt, A. Hill, A. Hale, M. Schilling, C. Boyd, S. Campbell, L. Dhar, A. Harris, High density, high performance optical data storage via volume holography: Viability at last?, *Opt. Quant. Electron.* 32 (1998) 393–404.
- [2] P. Gren, Four-pulse interferometric recordings of transient events by pulsed TV holography, *Opt. Lasers Eng.* 40 (2003) 517–528.
- [3] P. Saari, R. Kaarli, M. Ratsep, Temporally multiplexed fourier holography and pattern recognition of femtosecond-duration images, *J. Lumin.* 56 (1992) 175–180.
- [4] N.K. Nishchal, J. Joseph, K. Singh, Fully phase encryption using digital holography, *Opt. Eng.* 43 (2004) 2959–2966.
- [5] J.Y. Son, B. Javidi, K.D. Kwack, Methods for displaying three-dimensional images, *Proc. IEEE* 94 (2006) 502–523.
- [6] R.W. Smith, A note on practical formulas for finite ray tracing through holograms and diffractive optical-elements, *Opt. Commun.* 55 (1985) 11–12.
- [7] J.N. Latta, Computer-based analysis of holography using ray tracing, *Appl. Optics* 10 (1971) 2698–2710.
- [8] N. Yoshikawa, M. Itoh, T. Yatagai, Interpolation of reconstructed image in Fourier transform computer-generated hologram, *Opt. Commun.* 119 (1995) 33–40.
- [9] K. Nagashima, Improvement of reconstruction in 3D computer-generated holograms using 1D Fourier transform operations, *Opt. Laser Technol.* 33 (2001) 329–334.
- [10] L. Pugliese, G.M. Morris, Computer-generated holography in photorefractive materials, *Opt. Lett.* 15 (1990) 338–340.
- [11] K. Nakagawa, S. Iguchi, T. Minemoto, Computer generated holograms in photorefractive LiNbO<sub>3</sub> crystal, *Proc. SPIE* 3470 (1998) 77–83.
- [12] L. Dhar, A. Hale, H.E. Katz, M.L. Schilling, M.G. Schnoes, F.C. Schilling, Recording media that exhibit high dynamic range for digital holographic data storage, *Opt. Lett.* 24 (1999) 487–489.
- [13] M. Dubois, X.L. Shi, C. Erben, K.L. Longley, E.P. Boden, B.L. Lawrence, Characterization of microholograms recorded in a thermoplastic medium for three-dimensional optical data storage, *Opt. Lett.* 30 (2005) 1947–1949.
- [14] F. Mok, J. Diep, H.K. Liu, D. Psaltis, Real-time computer-generated holography by means of liquid-crystal television spatial light-modulator, *Opt. Lett.* 11 (1986) 748–750.
- [15] E.G. van Putten, I.M. Vellekoop, A.P. Mosk, Spatial amplitude and phase modulation using commercial twisted nematic LCDs, *Appl. Optics* 47 (2008) 2076–2081.
- [16] Y.J. Liu, X.W. Sun, Electrically switchable computer-generated hologram recorded in polymer-dispersed liquid crystals, *Appl. Phys. Lett.* 90 (2007) 191118.
- [17] Y.S. Ow, M.B.H. Breese, A.A. Bettioli, Proton beam writing for producing holographic images, *Nucl. Instrum. Methods Phys. Res., Sect. B* 267 (2009) 2289–2291.
- [18] D. Luo, X.W. Sun, Y.J. Liu, H.T. Dai, O.Y. Sheng, M.B.H. Breese, Z. Raszewski, Electrically switchable computer-generated hologram using a liquid crystal cell with a proton beam patterned polymethylmethacrylate substrate, *Appl. Optics* 48 (2009) 3766–3770.
- [19] M. Navarro, J.M. LopezVillegas, J. Samitier, J.R. Morante, J. Bausells, A. Merlos, Electrochemical etching of porous silicon sacrificial layers for micromachining applications, *J. Micromech. Microeng.* 7 (1997) 131–132.
- [20] T.E. Bell, P.T.J. Gennissen, D. DeMunter, M. Kuhl, Porous silicon as a sacrificial material, *J. Micromech. Microeng.* 6 (1996) 361–369.
- [21] P. Polesello, C. Manfredotti, F. Fizzotti, R. Lu, E. Vittone, G. Lerondel, A.M. Rossi, G. Amato, L. Boarino, S. Galassini, M. Jaksic, Z. Pastuovic, Micromachining applications of porous silicon, *Nucl. Instrum. Methods Phys. Res. B* 158 (1999) 173.

- [22] M.B.H. Breese, F.J.T. Champeaux, E.J. Teo, A.A. Bettiol, D.J. Blackwood, Hole transport through proton-irradiated p-type silicon wafers during electrochemical anodisation, *Nucl. Phys. B* 73 (2006).
- [23] V. Lehmann, The physics of macropore formation in low doped n-type silicon, *J. Electrochem. Soc.* 140 (1993) 2836–2843.
- [24] D. Mangaiyarkarasi, M.B.H. Breese, Y.S. Ow, C. Vijila, Controlled blueshift of the resonant wavelength in porous silicon microcavities using ion irradiation, *Appl. Phys. Lett.* 89 (2006).
- [25] E.J. Teo, A.A. Bettiol, P. Yang, M.B.H. Breese, B.Q. Xiong, G.Z. Mashanovich, W.R. Headley, G.T. Reed, Fabrication of low-loss silicon-on-oxidized-porous-silicon strip waveguide using focused proton-beam irradiation, *Opt. Lett.* 34 (2009) 659–661.
- [26] I. Rajta, S.Z. Szilasi, P. Fürjes, Z. Fekete, Cs. FeketDücsöe, Si micro-turbine by proton beam writing and porous silicon micromachining, *Nucl. Instrum. Methods Phys. Res. B* 267 (2009) 2292–2295.
- [27] E.J. Teo, D. Mangaiyarkarasi, M.B.H. Breese, A.A. Bettiol, D.J. Blackwood, Controlled intensity emission from patterned porous silicon using focused proton beam irradiation, *Appl. Phys. Lett.* 85 (2004) 4370–4372.
- [28] E.J. Teo, M.B.H. Breese, A.A. Bettiol, D. Mangaiyarkarasi, F. Champeaux, F. Watt, D. Blackwood, Multicolour photoluminescence from porous silicon using focused high-energy helium ions, *Adv. Mater.* 18 (2006) 51–55.
- [29] P. Mistry, I. Gomez-Morilla, R.C. Smith, D. Thomson, G.W. Grime, R.P. Webb, R. Gwilliam, C. Jaynes, A. Cansell, M. Merchant, K.J. Kirkby, Maskless proton beam writing in gallium arsenide, *Nucl. Instrum. Methods Phys. Res. B* 260 (2007) 437–441.
- [30] F. Menzel, D. Spemann, J. Lenzner, W. Bohlmann, G. Zimmermann, T. Butz, Fabrication of microstructures in III-V semiconductors by proton beam writing, *Nucl. Instrum. Methods Phys. Res. B* 267 (2009) 2321–2326.
- [31] D. Mangaiyarkarasi, O.Y. Sheng, M.B.H. Breese, B.L.S. Fuh, E.T. Xioasong, Fabrication of large-area patterned porous silicon distributed Bragg reflectors, *Opt. Express* 16 (2008) 12757–12763.
- [32] M. El Bouz, K. Heggarty, Signal window minimum average error algorithm for multi-phase level computer-generated holograms, *Opt. Commun.* 180 (2000) 21–28.